CENTER–TO–LIMB VARIATION OF THE STOKES V ASYMMETRY IN SOLAR MAGNETIC FLUX TUBES

M. Bünte, O. Steiner, and S.K. Solanki

Institute of Astronomy, ETH Zentrum, CH–8092 Zürich, Switzerland

Summary. The center–to–limb–variation (CLV) of synthetic Stokes V line profiles of the spectral line Fe I 5250.22 Å is presented and compared with observations. These synthetic profiles are calculated using models that contain the main features of the current basic picture of small scale magnetic fields on the sun. This *basic picture* consists of a flux tube in magnetohydrostatic equilibrium, which is separated from the surrounding non–magnetic atmosphere by a thin current sheet. Whereas the magnetic plasma is considered to be at rest the non–magnetic plasma is in convective motion which results in cool downflows along the flux tube boundary and warm upflows further away from it. The area asymmetry of Stokes V profiles observed at disk center can be explained by the presence of such non–magnetic downflows close to the boundary of the expanding flux tube . This mechanism also accounts for the unshifted zero–crossing wavelength of the Stokes V profiles. It is shown that the basic picture outlined above also reproduces the peculiar center–to–limb variation of the Stokes V asymmetry, in particular the sign reversal of the asymmetry near the limb (at $\mu \simeq 0.4$ for Fe I 5250.22 Å). The ingredients of the model mainly responsible for the sign reversal are identified. The fact that the agreement between theoretical and observational Stokes V profiles improves as more realistic features (like the temperature–velocity correlation of the granulation) are added to the model, leads us to conclude that the basic picture is correct and that the Stokes V parameter for small values of μ, i.e. near the limb, has the potential to serve as a sensitive diagnostic of convection in active regions.

1. Introduction

Although most of the photospheric magnetic fine structure can still not be spatially resolved by observations, it can be studied indirectly through the spectro–polarimetric signature of the Zeemann effect on atomic lines formed in photospheric magnetic fields. In this context the directly observable Stokes parameters I, Q, U, and V of a spectral line have proven to be a powerful tool in deriving semi–empirical models of photospheric magnetic elements in plages and the network (see reviews by Solanki, 1987b; Stenflo, 1989). Such investigations have led to the following basic picture of the photospheric magnetic field. It is thought to be concentrated into kilo Gauss flux tubes that are situated in the dark and downflowing intergranular spaces as a consequence of flux expulsion (see e.g. Schüssler, 1990). Although the individual flux tubes are surrounded by downflowing gas, there is no sizeable downflow within them. In the photospheric layers flux tubes spread rapidly with increasing height due to the exponentially decreasing gas pressure until they merge and fill almost the entire atmosphere above the merging height.

One remarkable feature of Stokes V profiles observed in active region plages and the quiet solar network is their pronounced asymmetry (Stenflo et al., 1984; Wiehr, 1985). Near disk center the area and amplitude of the blue wing exceed those of the red wing by several percent (Solanki and Stenflo, 1984), i.e. $\delta A = (A_b - A_r)/(A_b + A_r) > 0$ and $\delta a = (a_b - a_r)/(a_b + a_r) > 0$, where A_b, A_r denote the areas,

a_b, a_r the amplitudes of the blue and red wing, respectively. For LTE, Auer and Heasley (1978) have shown that the area asymmetry can only be explained in terms of velocity gradients. The first mechanism based on velocity gradients was proposed by Illing et al. (1975) and relied on the overlap of gradients in magnetic field strength and velocity. However, if we accept the current basic picture outlined above, in particular that the field strength decreases with height, then, as shown by Solanki and Pahlke (1988), a stationary flow within the magnetic flux tube implies a shift of the zero–crossing wavelength of the Stokes V profile larger than the observed upper limit of ± 250 ms^{-1} (Stenflo and Harvey, 1985; Solanki, 1986; Stenflo et al., 1987; Wiehr, 1987; Solanki and Pahlke, 1988). Other combinations of overlapping magnetic and velocity gradients have been proposed which can also produce asymmetric Stokes V profiles with only small zero–crossing shifts (Sánchez Almeida et al., 1988, 1989). However, such combinations invariably contradict the basic picture outlined above, since they require the field strength to increase with height. Van Ballegooijen (1985) pointed out that plasma flows in the *non–magnetic surroundings* of the flux tubes may also produce asymmetric Stokes V profiles. Grossmann–Doerth et al. (1988, 1989) then showed that if the velocity and the magnetic field are spatially separated, as proposed by Van Ballegooijen (1985), asymmetric, but unshifted, Stokes V profiles are produced.

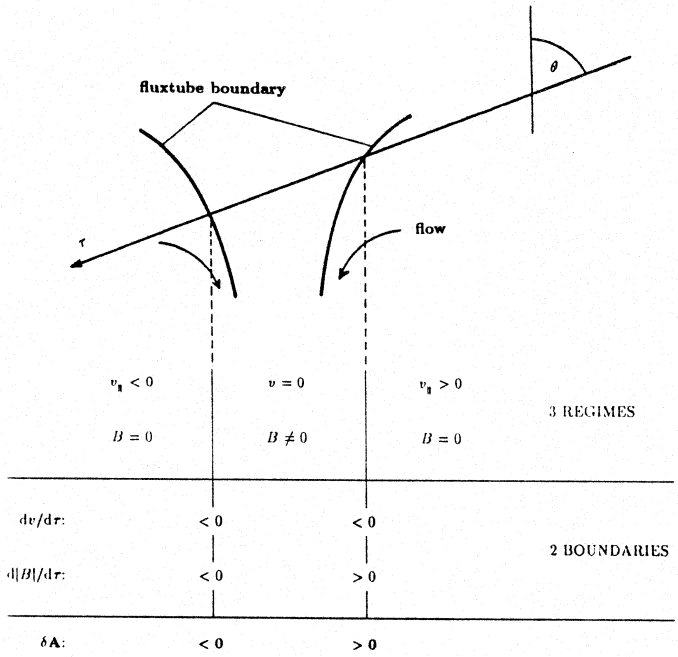

Fig. 1. Schematic illustration of the line of sight gradients of the magnetic and velocity fields for a highly inclined ray passing through a flux tube. According to Eq. (1) the contributions to the Stokes V asymmetry from the two intersections of the ray with the flux tube boundary counteract.

Solanki and Pahlke (1988) pointed out that the sign of the Stokes V area asymmetry depends on the signs of the line of sight gradients of the magnetic and the velocity fields alone:

$$\frac{d|\mathbf{B}|}{d\tau}\,\frac{dv(\tau)}{d\tau} \quad \begin{cases} < 0, & \Longrightarrow \quad \delta A > 0, \\ > 0, & \Longrightarrow \quad \delta A < 0. \end{cases} \tag{1}$$

Note that only the absolute value of the magnetic field is of importance, not its polarity, whereas the sign of the velocity plays a vital role. At solar disk center in the standard picture the observer's line of sights only pass from the magnetic into the non–magnetic atmosphere, but not the other way around.

Closer to the limb, however, a particular ray may cross the border between magnetic and non-magnetic regimes in both directions. Such a case is schematically illustrated in Fig. 1. If we assume the same velocity fields on both sides of the flux tube profile then the Stokes V asymmetries produced at the two interfaces will, in general[1], be of opposite sign. It is therefore not obvious whether the basic picture can account for the change in sign of the area asymmetry near the limb observed for Fe I 5250.22 Å by Stenflo et al. (1987) and for a larger sample of spectral lines by Pantellini et al. (1988). The aim of the present study is to find out under what conditions the area asymmetry changes sign near the limb. We also aim to obtain an idea of the diagnostic potential of the center-to-limb variation (CLV) of δA. In the present investigation we restrict our attention to the *area* asymmetry δA since the mechanism for its production at disk center is well understood. The *amplitude* asymmetry δa, in contrast, may be produced or changed by a much larger variety of causes (e.g. velocity changes along the line of sight, perpendicular to it, or in time, macroturbulence, etc.), so that its production, even at disk center, is still partially unclear.

2. The model

The basic structure of our model is shown in Fig. 2. A rotationally symmetric flux tube in magnetohydrostatic equilibrium is surrounded by non-magnetic plasma in stationary motion. The magnetic field is calculated by numerically solving the force balance equation including all tension forces. For further details regarding various aspects of the magnetohydrostatic solutions we refer to Steiner et al. (1986). We prescribe the gas temperature, pressure and density in the interior of the flux tube according to the plage model of Solanki (1986).

In the photosphere the magnetic pressure and the gas pressure are comparable in magnitude, i.e.

$$\frac{B^2}{8\pi} \simeq p_{\rm gas}. \tag{2}$$

For subsonic motions of a plasma with $v^2/C_s^2 = 2p_{\rm dyn}/(\gamma p_{\rm gas}) \ll 1$, the dynamic pressure is small compared to the gas pressure, so that by virtue of Eq. (2) the contribution of the former to the total pressure outside the flux tube can be neglected without changing the magnetic field structure noticeably. In the photosphere where typical maximal flow speeds are of the order of 10^5 cm/s this approximation seems to be justified which simplifies the numerical procedure considerably.

In the non-magnetic surroundings of the flux tube we initially prescribe an atmosphere similar to the quiet sun model, the HSRA (Gingerich et al., 1971), but systematically cooler by 300 K. Such an atmosphere provided the best fit to the observed δA values of four spectral lines at disk center (Solanki, 1989).

In addition various velocity fields are constructed which mimic some features of typical granular flow fields at various levels of sophistication. For example, we consider a pure downflow, following investigations of δA at disk center (Grossmann-Doerth et al., 1988, 1989; Solanki, 1989), or a purely horizontal inflow, i.e. a flow towards the flux tube axis. Of course, these velocity fields are unphysical, but help to identify some basic effects.

For a more physical representation, in a next step we calculate an irrotational downflow in the closer environment of the flux tube boundary (i.e. in a region $R(z) \le r \le [W + R(0)]/2$, where $R(z)$ is the flux tube radius at height z, $2W$ the distance between two neighbouring flux tubes, and $R(0)$ the radius at height $z = 0$, i.e. $\tau_{5000} = 1$ in the non-magnetic atmosphere at disk center). The flow pattern is determined by the equation of continuity which poses a nonseparable elliptic boundary value problem for the velocity potential (Bünte, 1989). For an adequate choice of the boundary conditions the resulting velocity field can serve as an approximation to the intergranular downflow resulting from convection models, such as those of Steffen et al. (1989), but at much lower computational costs.

[1] The velocity field must have sufficiently strong horizontal components for this to be valid.

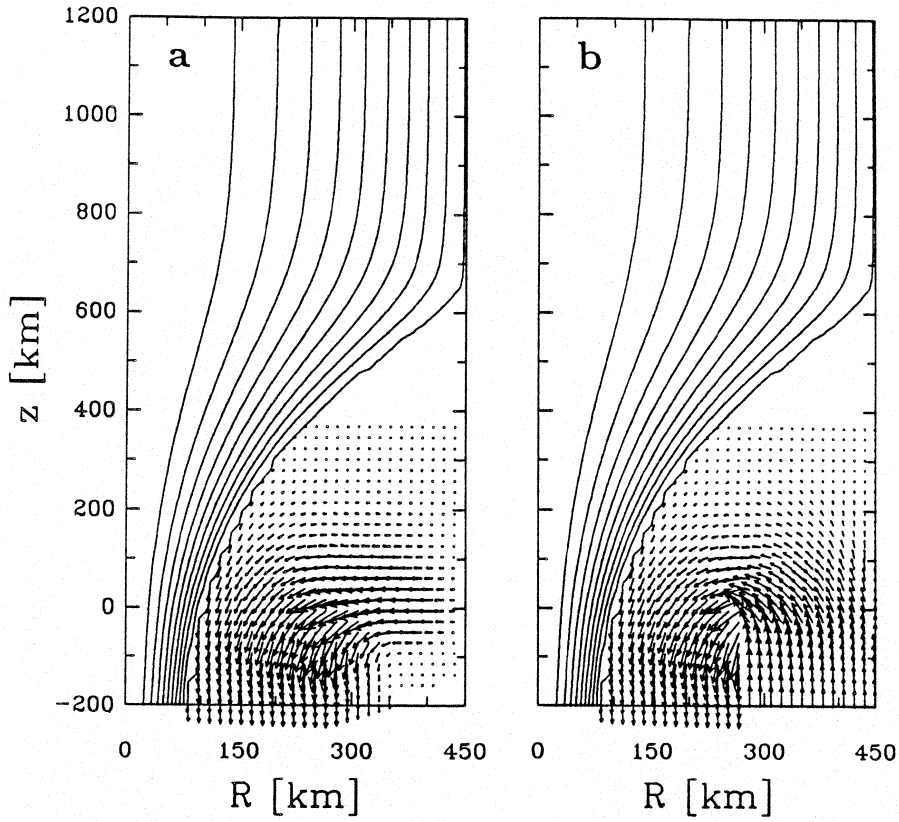

Fig. 2. Rotationally symmetric magnetic flux tubes in magnetohydrostatic equilibrium surrounded by non–magnetic plasma with two different stationary velocity fields. In Fig. 2a the flow is purely horizontal further away from the tube wall, whereas in Fig. 2b an upflow motion in that region prevails. Both flux tubes have a magnetic field strength of 1600 G, a radius of 100 km and a filling factor of 5 %. All these values refer to $z = 0$ ($\tau_{5000} = 1$ in the quiet sun at disk center). Maximum flow velocities are ≈ 4 km/s.

In the outer part of the non–magnetic region (i.e. for $[W + R(0)]/2 \leq r \leq W$) we either prescribe purely horizontal velocities which drop to zero at $r = W$ (the radial scale of our model), as shown in Fig. 2a, or an upflowing velocity field, which is simply the mirror–image of the downflow but with a reversed z–component (see Fig. 2b). The latter case very roughly resembles a granular flow pattern (Steffen et al., 1989) or the baroclynic convection cell bordering the flux tube model of Deinzer et al. (1984). As a final step in the direction of realism we have introduced a correlation between velocity and temperature. This correlation consists of a velocity dependent temperature rise in upflow regions, e.g. in the following way:

$$T(z) = \begin{cases} T^{*}_{\mathrm{HSRA}}(z), & \text{in downflow regions,} \\ T^{*}_{\mathrm{HSRA}}(z) + \dfrac{v_z}{v_{z\ \mathrm{max}}} \Delta T, & \text{in upflow regions,} \end{cases} \tag{3}$$

where $v_{z\ \mathrm{max}}$ is the maximum upflow velocity (typically ≈ 3.8 km/s) and $T^{*}_{\mathrm{HSRA}}(z) = T_{\mathrm{HSRA}} - 300$ K. For ΔT we have chosen values of typically 500 – 1000 K for consistency with the 3–D model calculations of Nordlund (1985, Fig. 4b) and the most recent 2–D results of Steffen (1990).

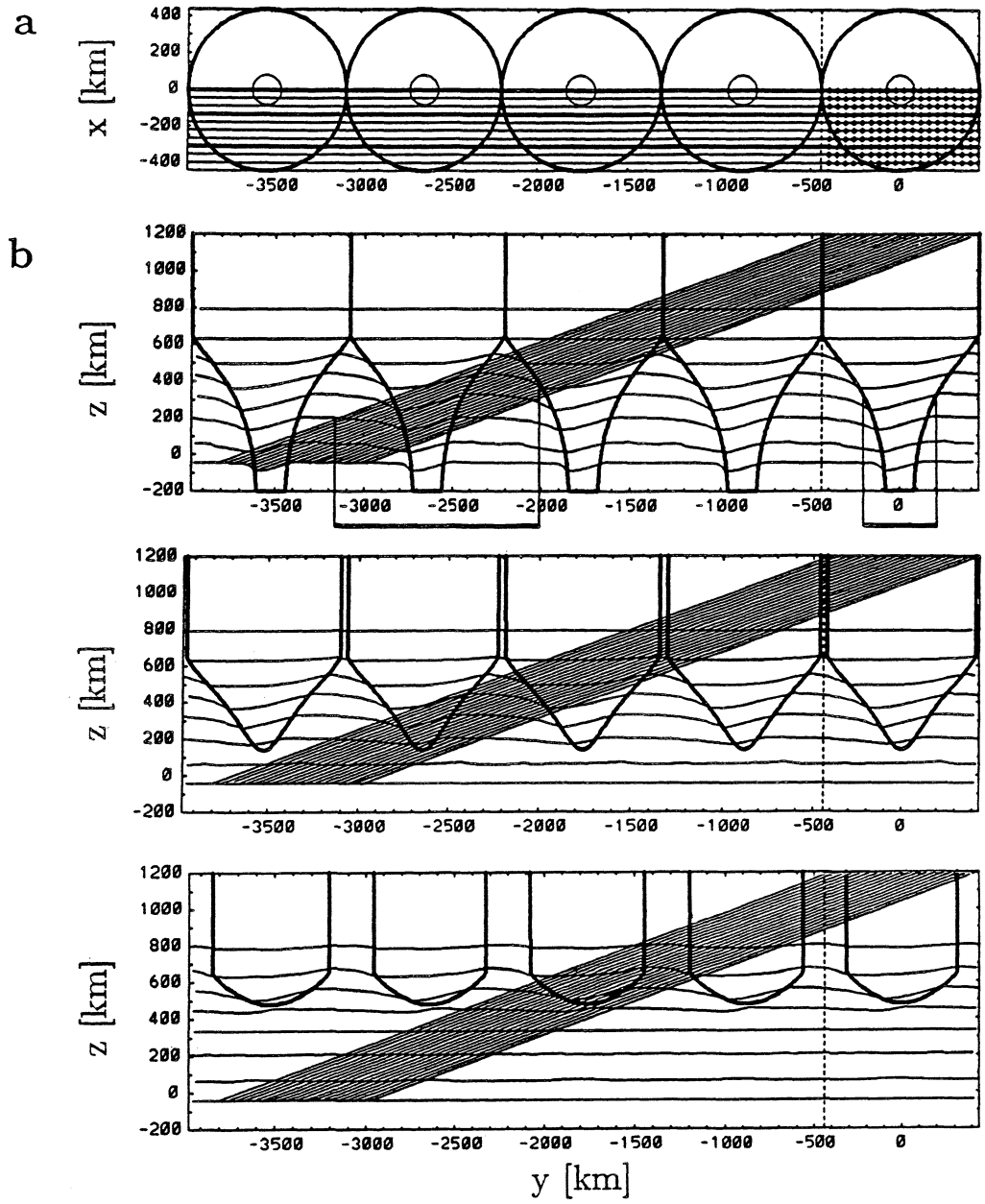

Fig. 3. Illustration of the model geometry for Stokes V calculations near the limb. a An array of merged flux tubes as seen from above (thick circles). Each horizontal line is the projection of a vertical plane cutting the model (the thick lines represent the planes shown in Fig. 3b). Each point to the right of the dashed line is the entry point into the top of the model of a ray lying in one of the vertical planes. b Illustration of the three vertical cuts that were indicated in Fig. 3a. The first frame represents the plane of symmetry (upper thick line in Fig. 3a), the middle and bottom frames correspond to the lower two heavy lines in Fig. 3a. The rays entering the model to the right of the dashed line for an "observation" close to the limb ($\theta = 70°$, i.e. $\mu = 0.34$) are visible as the group of slanted parallel lines. The thick lines are the contours where the flux tubes intersect with the vertical planes. The thin horizontal lines represent surfaces of equal optical depth τ, in steps of $\Delta \log \tau = 1$ from $\log \tau = -6.0$ to $+1.0$. For a spectral line which is formed in the layer $-3 \lesssim \log \tau \lesssim -1$ the horizontal range affecting Stokes V on both sides of a given flux tube is indicated below the first frame, for observations near the limb (left) and at disk center (right).

3. Calculation of the Stokes parameters at different disk positions

The computation of the hydromagnetic parameters (cf. Sect. 2) is followed by a *diagnostic procedure* which serves to determine the spectral signature of the model, i.e. the values of the emergent Stokes parameters. In the present contribution we are only interested in Stokes V.

The diagnostics involve two steps: (1) First the atmospheric quantities must be determined along a number of parallel rays (line of sight) passing at an angle θ (to the vertical) through the model. Only the line profiles averaged over all rays are finally compared with the spatially unresolved observations (1.5–D radiative transfer). Since flux tubes often come in groups we have assumed a periodic arrangement with a fixed filling factor at $z = 0$. This is an important aspect, since close to the limb a ray may pass through more than one single flux tube (see below). Fig. 3a shows the "merged" magnetic flux tubes from above. In reality, of course, flux tubes lose their identity as they merge, in particular the rotational symmetry breaks down and the field should also fill the gaps between the circles in Fig. 3a. However, the spectral line under consideration (Fe I 5250.22 Å) is formed in layers well below the height where merging occurs, so that the topological details of merging fields do not have to be taken into account.

A set of parallel planes, one of which contains the symmetry axes of the tubes, are chosen (indicated by the horizontal parallel lines). Each of the dots on these lines is the beginning of one particular ray which lies in the corresponding plane and forms an angle θ with the vertical of the atmosphere. Along each ray a set of points is chosen on the basis of an adaptive step size procedure with respect to the logarithm of the optical depth τ.

Fig. 3b shows sets of rays through three different planes of the model. The code used to place the rays and evaluate the atmospheric data along them is a greatly modified and extended version of the one described by Ringenbach (1987) and De Martino (1986). For the current work typically 10×19 rays are laid through the model (cf. Fig. 3a). In the following we consider a cluster of magnetic flux tubes with a field strength of 1600 G, a diameter of 200 km, and a filling–factor of 5%, all values given at $z = 0$. The fields merge at a height of approximately 650 km. The non–magnetic plasma in between the flux tubes is in stationary motion (with maximum velocities of ≈ 4 km/s).

(2) The Stokes parameters for a particular spectral line are calculated numerically in LTE along each ray using a code based on the one described by Beckers (1969 a,b). For more details, see Solanki (1987a). Finally, all the calculated profiles are added together. The resulting Stokes V profiles can be directly compared with observations.

4. Results

In the following we briefly describe the steps we have taken to test various mechanisms which may be responsible for the center–to–limb variation of δA.

(1) As θ is changed, so is the angle between the line of sight and the magnetic field, so that the π–component of the line becomes more prominent near the limb. It is this effect which is mainly responsible for the CLV of δA found by Auer and Heasley (1978). To test the importance of this effect we first calculated the CLV using the model described in Sect. 2, but with only pure downflows in the surroundings of the flux tubes, so that the observed δA at disk center is reproduced. This model completely fails to reproduce the observed CLV of δA. The calculated δA remains strictly positive and actually increases towards the limb.

(2) While observations at disk center are only sensitive to the *vertical* component of the velocity field its *horizontal* component becomes relevant for observations closer to the limb. Schüssler (1990) proposed that this is the main mechanism giving rise to the change in sign of δA. However, this is not a priori clear, since Fig. 1 illustrates that as one follows a typical line of sight the areas around the two points where it enters and leaves a flux tube give opposite contributions to δA. In this step we therefore considered a purely horizontal inflow in the non–magnetic surroundings of the tubes. Of course $\delta A = 0$ at $\mu = 1$. At the limb δA is small but positive in our calculations. We therefore conclude that

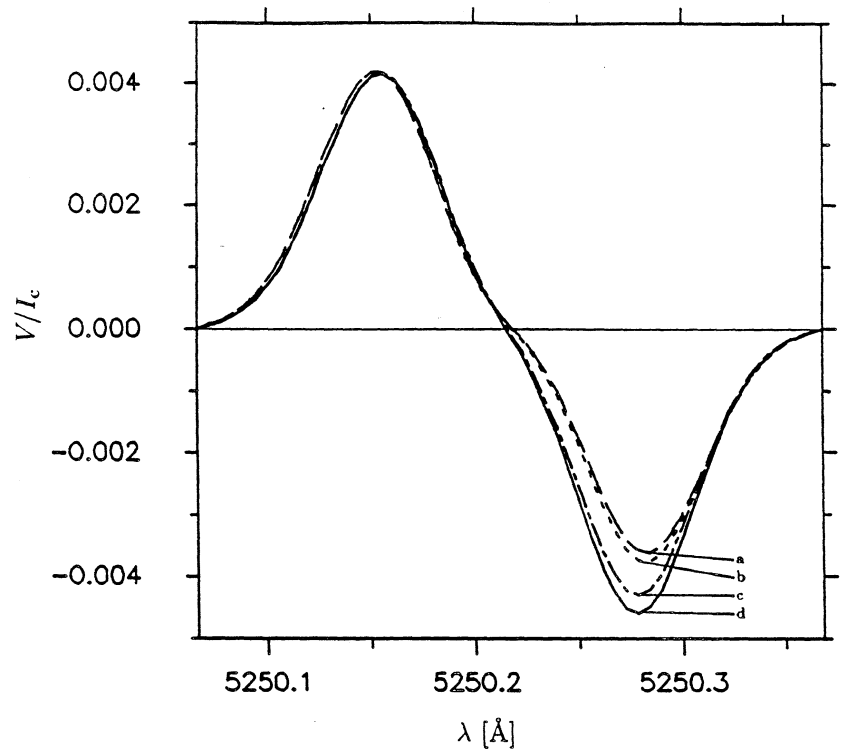

Fig. 4. Stokes V profiles of Fe I 5250.22 Å at $\theta = 70°$ ($\mu = 0.34$) arising from an array of flux tubes (see Figs. 2 and 3). Different profiles correspond to different velocity fields that were used in steps 1–6 (Sect. 4). Curve a: inflow and downflow without any upflow (step 3); curve b: upflow instead of inflow in the outer parts of the model (step 4), curve c: like curve b, but including a temperature–velocity–correlation (step 5), curve d: like curve c, but with enhanced horizontal velocity components (step 6).

the presence of a horizontal inflow by itself is not sufficient to produce the observed sign reversal, although it turns out to be a necessary ingredient (within the confines of the basic picture).

(3) In a third step we have combined an inflow with a downflow, as illustrated in Fig. 2a. Again, although the observations at disk center may be reproduced, the asymmetry does not change sign near the limb.

(4) Next an upflow has been introduced, leading to a model of type shown in Fig. 2b. This model, finally, reproduces the observed (positive) δA at disk center, and, at the same time, yields a negative δA near the limb. However, δA changes sign only very close to the limb ($\mu \approx 0.2$) for Fe I 5250.22 Å and does not drop below -1% to -2% for $\mu \gtrsim 0.1$, whereas observations show the sign reversal at $\mu \approx 0.4$ and values of -5% to -10% for $0.1 \leq \mu \leq 0.3$. Apparently some important ingredient is still missing in the models.

(5) In a next step a temperature–velocity–correlation of the type described in Sect. 2, Eq. (3) has been added, i.e. a warm upflow and a cool downflow. This model is able to produce both a large positive δA at $\mu = 1$ and a large negative δA for small values of μ.

(6) Finally, the behaviour of the asymmetry can be considerably influenced by changing the ratio of the maximum horizontal flow velocity to the maximum up–, respectively, downflow component. Enhanced horizontal velocities result in more pronounced negative values of δA near the limb if the temperature and the velocity are correlated as in step 5.

The effect on the line profile of some of the steps described above are illustrated in Fig. 4 which shows calculated Stokes V profiles of the line Fe I 5250.22 Å at $\mu = 0.34$, i.e. at an angle $\theta = 70°$. At this

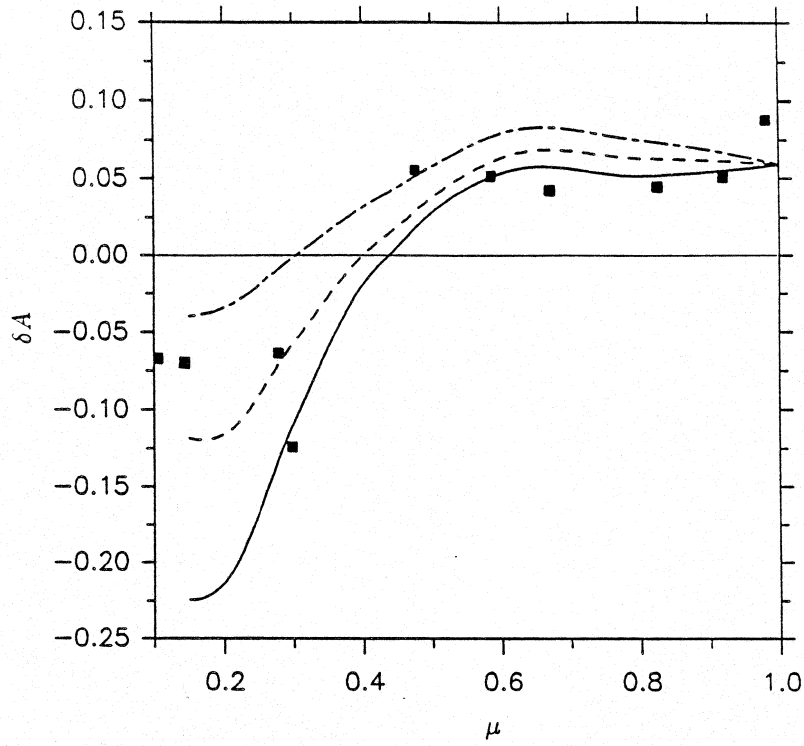

Fig. 5. Observed (squares) and calculated (curves) center–to–limb variation of the relative area asymmetry of Stokes V profiles of Fe I 5250.22 Å. The velocity fields used consist of a cool downflow near the flux tube boundary and a warm upflow further away from it (dashed curve, step 5). The dot–dashed curve results for suppressed, the solid curve for enhanced horizontal velocities (step 6).

position on the solar disk (close to the limb) the area asymmetry of the *observed* Stokes V profile has already changed sign, i.e. the red wing dominates the blue. The synthetic profiles in Fig. 4 all result from the same magnetic field configuration but from different velocity fields in the non–magnetic atmosphere between the flux tubes. Curve a represents the results from step 3, curve b corresponds to step 4, curve c to step 5 (where in comparison to step 4 a temperature–velocity–correlation has been introduced), and curve d shows the effect of enhancing the horizontal velocities by a factor of two while leaving the vertical components and the associated temperature structures unchanged (step 6).

Having identified some of the main parameters controlling the CLV and the sign reversal of δA, we have compared the synthetic profiles with the observations. Only the results of steps 5 and 6 are discussed further. Fig. 5 shows the observed (squares, data taken from Stenflo et al., 1987) and calculated relative area asymmetry of the Stokes V profiles of the line Fe I 5250.22 Å as a function of $\mu = \cos\theta$. The dashed curve corresponds to the $\delta A(\mu)$ produced with the model of step 5. The maximum horizontal inflow is 2.9 km/s, the maximum vertical velocity components are 3.8 km/s. The ΔT parameter of Eq. (3) is chosen to be 1000 K. The solid curve results when the horizontal velocity component is enhanced by a factor of 2, while the dot–dashed curve is obtained if the horizontal velocity is reduced by the same factor. The correspondence of these models to the observations is gratifying.

5. Conclusions

The center-to-limb variation of synthetic Stokes V line profiles of the spectral line Fe I 5250.22 Å has been investigated. The underlying hydromagnetic model consists of a cluster of rotationally symmetric magnetic flux tubes surrounded by granular non-magnetic plasma in stationary motion. From the variation of the velocity fields we come to the following conclusions:

1. Velocity fields in the *non-magnetic* environment are able to quantitatively reproduce not only the observed Stokes V area asymmetry (δA) of Fe I 5250.22 Å at disk center, but also its center-to-limb variation including the sign reversal of the asymmetry around $\mu = 0.4$ ($\theta \simeq 60°$).
2. The closer the assumed non-magnetic atmospheric dynamics (in the environment of the flux tubes) correspond to the solar granulation (i.e. warm central upflows, strong horizontal velocities, and cool downflows), the better the observed center-to-limb behaviour of the Stokes V asymmetry δA is reproduced. This is a sign that the basic picture of magnetic flux tubes and of their relations to the surroundings outlined in Sect. 1 is correct.
3. The center-to-limb variation of the area asymmetry of Stokes V profiles can be used as a sensitive tool for investigating the velocity and temperature structure of the granulation in solar active regions.
4. The temperature-velocity-correlation of granular convective motions is an essential ingredient for reproducing the observed δA away from disk center.
5. The calculated line profiles do not show any shift of the zero-crossing wavelength at any position on the disk, in agreement with the observations of Stenflo et al. (1987), Pantellini et al. (1988), and Wiehr (private communication). This is a direct result of the fact that the present models do not include any velocity within the magnetic features. As proved by Grossmann-Doerth et al. (1988, 1989) such a segregation of velocity and magnetic fields always leaves the V profiles unshifted, irrespective of the geometrical details. However, we do foresee possible problems for mechanisms which make use of velocities within the flux tubes to produce a non-zero δA and rely on special geometries to keep the zero-crossing shift small, since the geometry of the field and of the velocity along the line of sight is strongly dependent on θ. For example, near disk center the main contribution to the Stokes V signal comes from rays which remain completely within the magnetic features (Solanki, 1989), whereas near the limb every ray passes at least partially through the non-magnetic atmosphere.

Acknowledgements. We thank J.O. Stenflo for helpful discussions and careful reading of the manuscript. The work of two of us (M.B. and O.S.) has been supported by grant No. 20-26'436.89 of the Swiss National Science Foundation.

References

Auer, L.H., Heasley, J.N.: 1978, *Astron. Astrophys.* **64**, 67.
Beckers, J.M.: 1969a, *Solar Phys.* **9**, 372.
Beckers, J.M.: 1969b, *Solar Phys.* **10**, 262.
Bünte, M.: 1989, *Diplomarbeit*, ETH Zürich.
Deinzer, W., Hensler, G., Schüssler, M., Weisshaar, E.: 1984, *Astron. Astrophys.* **139**, 435.
De Martino, S.: 1986, *Diplomarbeit*, ETH Zürich.
Gingerich, O., Noyes, R.W., Kalkofen, W., Cuny, Y.: 1971, *Solar Phys.* **18**, 347.
Grossmann-Doerth, U., Schüssler, M., Solanki, S.K.: 1988, *Astron. Astrophys.* **206**, L37.
Grossmann-Doerth, U., Schüssler, M., Solanki, S.K.: 1989, *Astron. Astrophys.* **221**, 338.
Illing, R.M.E., Landman, D.A., Mickey, D.L.: 1975, *Astron. Astrophys.* **41**, 183.

Nordlund, Å.: 1985, in H.U. Schmidt (Ed.), *Theoretical Problems in High Resolution Solar Physics*. Max Planck Inst. f. Astrophys., München, p.1.
Pantellini, F.G.E., Solanki, S.K., Stenflo, J.O.: 1988, *Astron. Astrophys.* **189**, 263.
Ringenbach, A.: 1987, *Diplomarbeit*, ETH Zürich.
Sánchez Almeida, J., Collados, M., Del Toro Iniesta, J.C.: 1988, *Astron. Astrophys.* **201**, L37.
Sánchez Almeida, J., Collados, M., Del Toro Iniesta, J.C.: 1989, *Astron. Astrophys.* **222**, 311.
Schüssler, M.: 1990, in J.O. Stenflo (Ed.), *Solar Photosphere: Structure, Convection, and Magnetic Fields*, IAU Symp. **138**, 161.
Solanki, S.K.: 1986, *Astron. Astrophys.* **168**, 311.
Solanki, S.K.: 1987a, Ph.D. Thesis, ETH Zürich.
Solanki, S.K.: 1987b, in E.-H. Schröter, M. Vázquez, A.A. Wyller (Eds.), *The Role of Fine-Scale Magnetic Fields on the Structure of the Solar Atmosphere*, Cambridge University Press, p.67.
Solanki, S.K.: 1989, *Astron. Astrophys.* **224**, 225.
Solanki, S.K., Pahlke, K.D.: 1988, *Astron. Astrophys.* **201**, 143.
Solanki, S.K., Stenflo, J.O.: 1984, *Astron. Astrophys.* **140**, 185.
Steffen, M.: 1990, in L. Crivellari, I. Hubeny (Eds.), *Stellar Atmospheres: Beyond Classical Models*, Kluwer, Dordrecht, (in press).
Steffen, M., Ludwig, H.-G., Krüß, A.: 1989, *Astron. Astrophys.* **213**, 371.
Steiner, O., Pneuman, G.W., Stenflo, J.O.: 1986, *Astron. Astrophys.* **170**, 126.
Stenflo, J.O.: 1989, *Astron. Astrophys. Rev.* **1**, 3.
Stenflo, J.O., Harvey, J.W.: 1985, *Solar Phys.* **95**, 99.
Stenflo, J.O., Harvey, J.W., Brault, J.W., Solanki, S.K.: 1984, *Astron. Astrophys.* **131**, 33.
Stenflo, J.O., Solanki, S.K., Harvey, J.W.: 1987, *Astron. Astrophys.* **171**, 305.
Van Ballegooijen, A.A.: 1985, in H.U. Schmidt (Ed.), *Theoretical Problems in High Resolution Solar Physics*, Max Planck Inst. f. Astrophys., München, p.177.
Wiehr, E.: 1985, *Astron. Astrophys.* **149**, 217.
Wiehr, E.: 1987, in J.L. Linsky, R.E. Stencel (Eds.) *Cool Stars, Stellar Systems, and the Sun, V.*, Lecture Notes in Physics Vol. 291, Springer Verlag, Berlin, p.54.

Discussion

J.C. Henoux: What temperature difference did you assume?

S. Solanki: We assumed a maximum temperature difference of 1000° K between the up- and the downflowing part of the non-magnetic atmosphere at equal geometrical height. The difference at equal optical depth is smaller. This temperature difference lies well within the maxima and minima of temperatures plotted by Nordlund (1986, Sac Peak Conference) from a scan through his models.

B. Lites: Are size scales for the "upflow/downflow" regions surrounding the flux tube and their signature in white light consistent with the flux tube residing in an intergranular lane?

S. Solanki: Yes. For the model I have shown the horizontal size of the full "granule" is approximately 700-800 km, which corresponds to about the size of a small or abnormal granule, as observed in active regions. However, we do intend to look at models with other flux tube diameters and other sizes of "granular" cells.

D. Deming: The 5-minute oscillation is prominent in field-free regions, and is known to produce "velocity/intensity" correlations in spectral lines. Can it play a role in Stokes V asymmetries?

S. Solanki: In active regions the 5-minute oscillations have an amplitude of approximately 250 m/s, while we require velocities of approximately 1 km/s to reproduce the asymmetry. I therefore feel that the 5 minute oscillations do not have a significant effect on the asymmetry, although they probably do affect the details.

S. Koutchmy: The lifetime of a magnetic flux tube region is large compared to the lifetime of a bright granule which would show the velocity pattern you need in your model. Additionally, your model is magnetostatic and moreover stationary; accordingly — for self-consistency — the flux tube should be stable or

at least should not rise quickly due to instability. Obviously, this cannot be the case when large velocity gradients are present near the tube, especially for velocities directed perpendicular to the magnetic field lines!

A. Skumanich: Does your model predict a bright ring around the flux tube region at the center of the disc?

S. Solanki: First to answer your question: No, our model does not predict a bright ring around the flux tube. Rather, it predicts that the bright flux tubes are embedded in cool, i.e. dark, intergranular lanes. To your comment, Serge: Our calculations are a simple approach to try to reproduce a substantial body of data, i.e. FTS Stokes V spectrum of active regions (note, that the small models simultaneously also reproduce many other spectral diagnostics). These observations are spatially and temporally averaged, so that the models also represent an "average" magnetic element. As for as the stability of flux tubes is concerned, the question is not completely resolved. However, calculations including velocities in the surroundings of magnetic elements do suggest that they can be stabilized by external flows. I suggest that you read the paper by Schusler (*Astron. Astrophys.*, 1984).

R. Canfield: What are the free parameters of your models?

S. Solanki: The magnetic free parameters are the field strength and horizontal profile at one height. They have been chosen to correspond to observations. The temperature specifications have whenever possible been taken from empirical models. The velocity profile is prescribed at the boundary. We have used a couple of different profiles, but found no great difference in the profiles. I feel this is due to the fact that close to the limb the Stokes V profile "feels" a large horizontal region around the magnetic features.

L. November: Koutchmy observes fine-structure unresolved in the vicinity of flux tubes. Your model is not unique. Is it possible that spatially unresolved elements could also produce the observed V asymmetry and sign reversal near the limb?

S. Solanki: One of the things we have learned from this investigation is that the change in sign of the area asymmetry near the limb is a subtle effect due to the balancing of the asymmetry produced at two different boundaries between the magnetic and the non-magnetic atmosphere. It is therefore very difficult, if not impossible, to tell how the asymmetry will behave in a qualitatively different model, without a complete numerical calculation.

S. Koutchmy: I am referring to the Larry November question which is addressing the problem of including the red-shifted mixed polarity of the weak field "contained" in the region of the flux tubes of dominant polarity. Either this spatial mixing effect or the fast decrease of the mixed polarity with height will show a reversing of the sign of the blue-red asymmetry when you go to the limb or when magnetograms made in a photospheric line are compared to magnetograms taken just above in the low chromosphere (B_2 line of MgI). At the photospheric level the area asymmetry is obviously a result of the very complicated pattern we have among the flux tubes region: a strong unshifted field and red-shifted weak field of the mixed polarity, and a variation with heights. Accordingly, the "blue/red" asymmetry of Stokes parameters is a good diagnostic also for high spatial resolution observations.

S. Solanki: I'm afraid I do not understand the mechanism you propose to produce a sign reversal of the area asymmetry. As I already pointed out to Larry November, it is not currently possible to say without a proper calculation whether a particular model (including yours) will produce a sign reversal. I personally believe in Ockham's razor, i.e. we keep a model as simple as possible as long as there is no very compelling reason to make it more complex. I feel that the reality of small scale mixed polarities can only be firmly established by IR observations.

J.C. Henoux: Is the 1000° K temperature difference you used in agreement with other observations?

S. Solanki: I don't know, but it is probably quite difficult to determine the true velocity in granules from observations. We have also calculated a model with a difference of 500° K and have also obtained the sign reversal, although we did not reproduce the data as well. But we need to do more calculations.